Method of numerical simulation flow on rough Cartesian calculation grids

V A Sereda

Research Institute of Problems Physical Modelling Kharkiv Aviation Institute, NationalAerospaceUniversity “Kharkiv Aviation Institute”, 17 Chkalova str., Kharkiv 61070, Ukraine

E-mail: v.sereda@khai.edu

Abstract. The use of an unstructured computational grid in computational aerohydrodynamics is associated with a number of difficulties: the non-conservativeness of the momentum balance equation, the manifestation of nonphysical grid effects, a decrease in the time step for the Courant-Friedrichs-Levy condition, and the complexity of modeling a dynamic grid. Of course, these difficulties are solvable, however, they require complex logic of mathematical algorithms, which leads to an increase in the requirements for the resource of the software product. Therefore, the author cultivates a low-resource method for calculating currents on coarse calculated Cartesian grids. This method has the same logic for the entire computational domain, but it requires solving the problem of flow turning in places with complex geometry. To calculate flows on rough Cartesian computational grids, the method of isentropic rotation of the flow in cells adjacent to the surface is proposed. The structure of the computational domain with masks of the guiding properties and the adjacent layer is described. The algorithm of isentropic rotation of the flow using the method of features is given. An algorithm is described for the effect of the wall on the intensity of the features involved in the rotation of the flow.

1. Introduction
Most of the problems of computational fluid dynamics are related to the study of objects of complex geometry. To simulate the flow around such objects, adaptive irregular meshes are often used [1, 2]. However, such grids require the involvement of complex logic of computational algorithms and increased computer performance. Therefore, rectangular grids [3-5] look more attractive, which do not require bulky arrays of nodes and are compatible with the capabilities of ordinary computers. A universal method for constructing solutions on coarse regular grids is the singularity method [6, 7]. To set the localization of these features and describe their “power”, the so-called “gas-dynamic mask” can be used.

2. Methods
The method was tested in the author’s software package for modeling the unsteady flow of a viscous compressible gas. The package was developed in Fortran 90 and contains a mask generator, calculation module and graphical interface. The mask generator includes a graphic module for 2D layering and editing of the results of creating masks (Fig. 1). To obtain the geometry of the object of

study, a 3D model in the STL format is used, which can be obtained in any third-party CAD application.

The process of motion of a viscous heat-conducting medium is displayed by the matrix of states of physical fields $\overline{\Pi}(\vec{x}, t) = \{p, \rho, \vec{w}\}(\vec{x}, t)$ (where, $\vec{x} = \{x_1, x_2, x_3\}$ – coordinate vector; $\vec{w} = \{w_1, w_2, w_3\}$ – velocity vector), defined by the conservative form of writing the system of equations of gas dynamics:

$$\frac{\partial \overline{F}}{\partial t} + \vec{\nabla} \vec{\overline{\Phi}} = \sum_{n=1}^{M_S} \left(\frac{\partial \overline{F}}{\partial t} \right)_{(n)} + \sum_{n=1}^{M_F} \overline{\Delta}_{(n)} , \tag{1}$$

where, $\overline{F} = \rho \left\{ 1, S, \vec{w}, \varepsilon^0 \right\}$ is generalized stream vector matrices; $\vec{\nabla} = \vec{i}_k \frac{\partial}{\partial x_k}$ is Hamilton operator; $\vec{\overline{\Phi}} = \sum_{k=1}^{3} \vec{i}_k \overline{\Phi}_k$ is vector-matrix of convective and wave processes; $\overline{\Phi}_k = \overline{F} w_k + p\left(0, 0, \delta_{1,k}, \delta_{2,k}, \delta_{3,k}, w_k\right)$ is projections of the vector matrix of convective and wave processes on the coordinate axis; $\overline{\Delta}_{(n)} = \left\{ 0, \frac{\partial(\rho S)}{\partial t}, \vec{f}, \frac{\partial\left(\rho \varepsilon^o\right)}{\partial t} \right\}_{(n)}$ is vector-matrix of "free" sources-sinks; $\vec{f} = \{f_1, f_2, f_3\}$ is vector of intensity of the field of mass forces; M_S is the total number of sources-sinks groups due to the substantial transfer; M_F is the total number of groups of "free" sources-sinks.

The solution of the system of equations describing gas-dynamic flows is performed using the finite-difference method modified for boundary nodes by S K Godunov [8]. To determine the fluxes between internal cells, the solution of the problem of the decay of an arbitrary discontinuity is used. Near solid walls, the problem of the interaction of a gas flow with an obstacle is solved. At the boundary nodes of the computational domain, a solution of the form of a Riemannian rarefaction wave is used.

Various factors perturbing the main flow are modeled by the method of features of the type of sources-sinks associated with mass transfer and free. The qualitative composition of sources and sinks and the corresponding mathematical representations are given in table. As a one-parameter model of turbulence, the approximation viscosity standardization method is used [9]. For this, the entropy transfer equation has been added to the system. In addition, viscous friction forces are modeled by adding to the right sides of the momentum equations the components of the strain rate tensor in the form of a perturbation of the main solution.

Table. "Element base" of the model

Intensities of generating factors (components)	Record form	Mechanism of action (transfer)
Source of mass	$\frac{\partial \rho_{(1)}}{\partial t}$	substantial
Frictional forces	$\frac{\partial (\rho S)_{(2)}}{\partial t}$	free
Normal tensions	$\overline{\Delta}_{I\,(3)}$	
Tensions of surface forces	$\overline{\Delta}_{I\,(4)}$	
Inertia tensions	$\overline{\Delta}_{I\,(5)}$	
Energy source (heat supply)	$\frac{\partial \left(\rho \varepsilon^o\right)_{(6)}}{\partial t}$	substantial

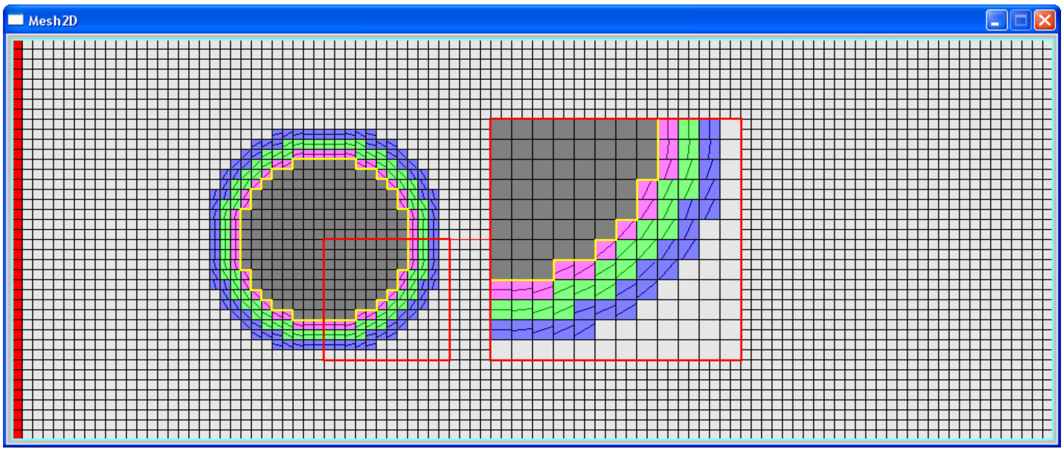

Figure 1. Display of the structure of the computational domain in the mask generator: cyan – boundaries of the computational domain; black – computational cell boundaries; yellow – surface mask; blue/green/red – guide cosine mask; ■ – volume mask; ■ – computational cell; ■ – features of the type sources-drains; ■, ■, ■ – adjoining layer mask.

To describe the topology of the object of study in the computational domain on a regular rectangular grid, two types of masks are used: volume and surface. The volume mask is used to model solids that completely occupy the internal volume of the cell and therefore are excluded from the solution area. The surface mask is used to model thin-walled structural elements and serves to separate cells that do not communicate with each other.

Modeling of smooth flow is carried out using two types of masks: guide cosines and the adjacent layer. The mask of guiding cosines contains an array of averaged normals to the curved solid-state surface of the original [10-12]. The mask of the adjacent layer shows the distance from the streamlined surface and sets the intensity of the influence of the cosine mask.

In cells where the cosine mask is not zero (if mask_cosin(i, j, k) $\neq 0$), an isentropic rotation of the flow is performed in the direction perpendicular to the averaged normal vector. The rotation of the flow is subject to the conservation of the kinetic energy of the flow in the cell before and after the rotation. For this, the angle α between the velocity vector $\vec{w}$ and the tangent to the surface vector $\vec{\tau}$ perpendicular to the averaged normal vector is determined $\vec{n}$. Next, the vector $\vec{w}$ is projected onto the vector $\vec{\tau}$, and the main direction $\vec{\tau}$ of the flow is selected for the direction:

$$\begin{cases} w_1 = |w| \sin \alpha; \\ w_2 = |w| \cos \alpha. \end{cases} \tag{2}$$

In addition, in the first adjacent layer (if mask_label (i, j, k, 1) = 1), the isoentropic approximation of the solution of the problem of the interaction of gas with an obstacle is also used. In subsequent layers, the influence of the mask of guiding cosines weakens, which is expressed by turning the flow not at the full angle α, but at its fraction r. The angle fraction is determined depending on the layer (l = 1...N, where, N is the number of layers) and is calculated by the Gaussian distribution, similar to the SPH method [13-15]:

$$r(l) = \frac{1}{\pi} e^{-\frac{(l-b)^2}{2N^2}}, \tag{3}$$

where, l is layer number; b is wall influence coefficient (>10).

Like SPH methods, the smoothing length is the thickness of the mask of the adjacent layer mask_label(i, j, k, l) and is calculated as hN (where h is the spatial integration step). In the case of using a movable mask, which moves along the OX axis with a velocity u, it is necessary to recalculate the internal energy, and then the temperature and pressure:

$$\varepsilon = \varepsilon^0 + \left(w_1 - w_1^0\right)u , \quad (4)$$

where, ε^0 is internal energy before the flow turns; w_1^0 is substantial velocity along the axis OX (in direction 1) before the flow turns.

3. Results

To test the method, we simulated the flow around an infinite cylinder on a computational grid of 100×40×1 with a Reynolds number of 112. In Fig. 2, in the form of color maps of physical fields, the phase of establishing the flow around the cylinder is displayed. When flowing around, a boundary layer is detached (at point C) with the formation of a stagnant zone in which two symmetric stationary vortices exist stably.

This is shown in Fig. 3 diagram of streamlines. The use of masks in combination allows one to obtain the adhesion of the flow to the surface of the cylinder on a low-resource coarse mesh. Without using the proposed method, flow separation occurs much earlier (at point O) (see physical fields of concentration of fresh air charge).

In Fig. 4 shows a plot of velocity vectors when flowing around a cylinder using a single-layer cosine mask. The plot shows the absence of a blow against the wall, despite the use of a fairly coarse mesh. The presence of a mask affects nearby cells and provides a smooth change in the direction of the velocity vectors around the surface of complex geometry. The cosine mask has the greatest influence on the flow pattern (Fig. 4) and quantitative parameters (Fig. 5) in the front of the cylinder, i. e., at the point where the flow hits the wall.

In Fig. 5 shows the distribution of the components of the velocity vector over the upper and lower surfaces of the cylinder relative to the plane of symmetry. The graph shows a monotonic change in both components of the velocity vector when using the cosine mask (pos. 2). Thus, the proposed measures allow for a smooth flow around roughly approximated objects, and more accurately find their integral characteristics (for example, aerodynamic coefficients).

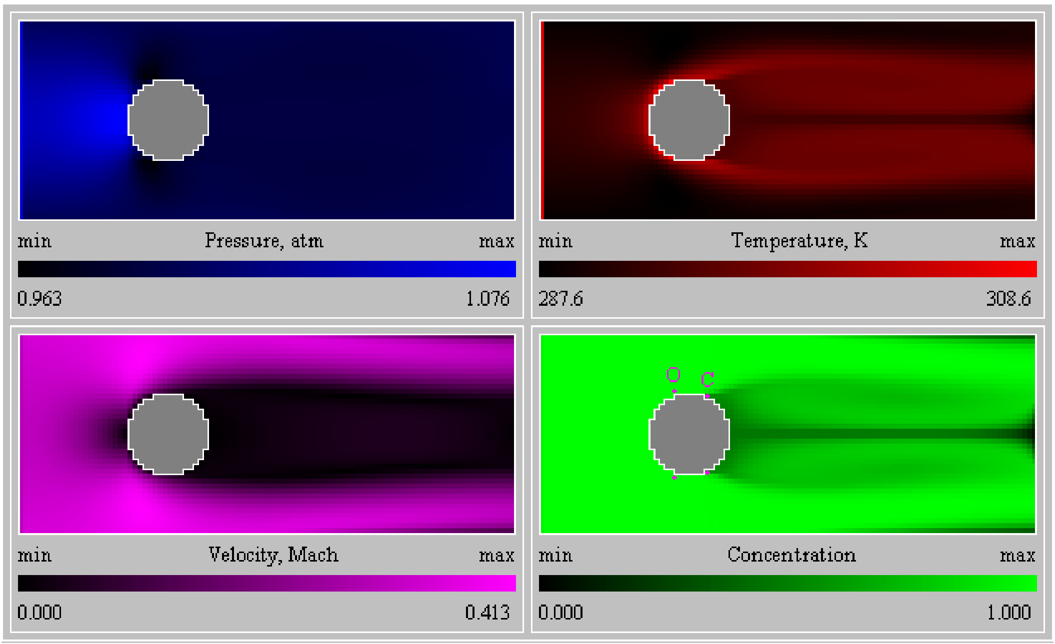

Figure 2. Fields of physical parameters when flowing around an infinite cylinder at Re=112 using a mask of guide cosines.

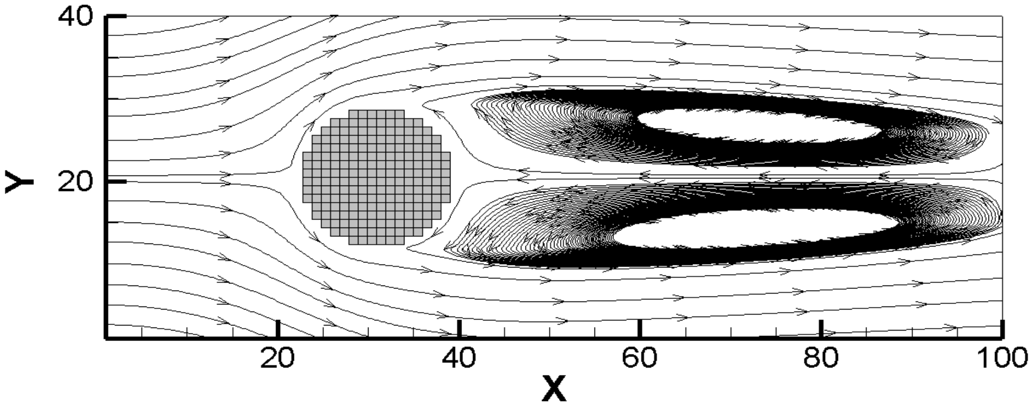

Figure 3. Diagram of streamlines.

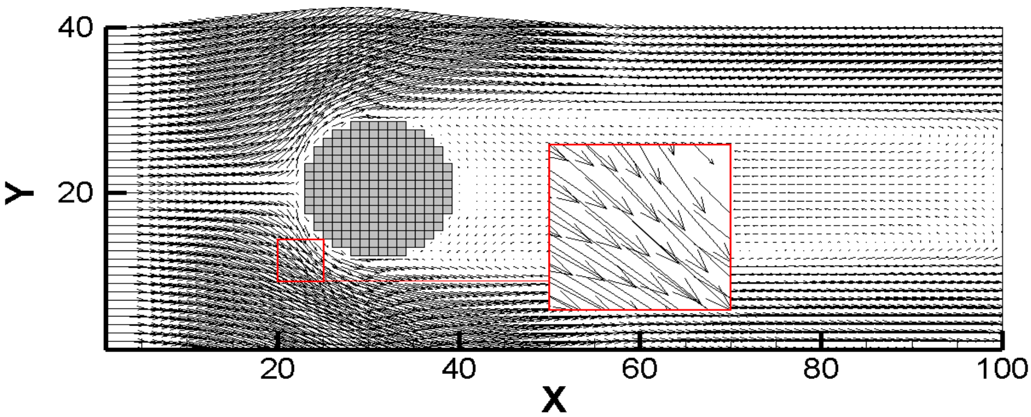

Figure 4. Diagram of velocity vectors.

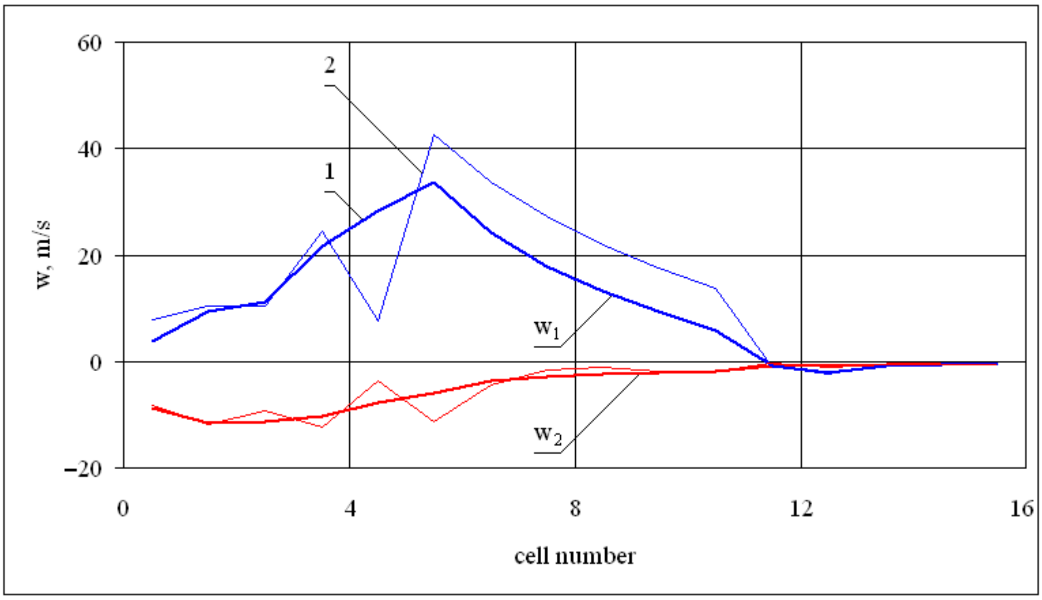

Figure 5. Distribution of velocity components over the surface of the cylinder: 1 – using a mask of guide cosines, simulating the effect of the walls of the cylinder on the flow; 2 – without using a mask.

4. Conclusion

The use of masks with special properties requires the development of specialized (for the applicable calculation package) grid generators, which is a separate non-trivial task. The use of the mask of guiding cosines together with the mask of the adjacent layer make it possible to obtain a physical picture of the flow around using a rough Cartesian regular grid. When the mesh thickens, the mask of the adjacent layer allows you to simulate the boundary layer, setting each cell with the parameters of the displacement thickness, loss of momentum and energy.

References

[1] Wang Z J 2011 *Adaptive High-order Methods In Computational Fluid Dynamics* (Singapore: World Scientific) p 460

[2] Myong H K and Kim J 2006 Development of a flow analysis code using an unstructured grid with the cell-centered method. *Journal of Mechanical Science and Technology.* № 20 pp 2218-2229

[3] Lopez J, Hernández J, Gomez P and Faura F 2013 *A two-grid adaptive volume of fluid approach for dendritic solidification* (Computers & Fluids) № 86 pp 326-342

[4] Wackers J, Leroyer A, Deng G and Queutey P 2012 *Adaptive Grid Refinement for Hydrodynamic Flow Simulation* (Computers & Fluids) № 55 (4) pp 85-100

[5] Afendikov A L, Khankhasaeva Ya V, Lusky A E, Menshov I S and Merkulov K D 2016 *Computation and Visualization of Flows Past Bodies in Mutual Motion* (Scientific Visualization) № 4 (8) pp 128-138

[6] Munson B R, Okiishi T H, Huebsch W W, Rothmayer A P 2012 *Fundamentals of Fluid Mechanics* (New York: John Willey & Sons. Inc.) 7th Edit. p 792

[7] Moffatt K 2009 Singularities in Fluid Dynamics and their Resolution (Lecture Notes in Mathematics) pp 157-166

[8] Ambrozhevich A V 2005 Numerical modeling of thermophysical processes in engine building (Kharkov: KhNADU) p 77

[9] Boychuk I P 2012 *Method Complex Aerodynamic Modeling of Freely Flying System "Glider-Engine"* (Kharkov: NAU "KhAI") diss. cand. tech. sciences, p 221

[10] Ambrozhevich A V, Boychuk I P, Larkov S N and Sereda V A 2008 *A low-resource method for numerical modeling of flows in geometric regions of complex shape* (Aerospace engineering and technology) № 6 (53) pp 45-53

[11] Ambrozhevich A V, Boychuk I P, Migalin K V and Sereda V A 2012 *Numerical study of a complex of processes of external and internal flow around an unmanned aerial vehicle with an ejector ramjet engine* (Aerospace engineering and technology) № 1 (78) pp 59-62

[12] Ambrozhevich M V, Kornev A V and Sereda V A 2016 *Low-resource Turbojet Engine Sub-model* (Aerospace engineering and technology) № 1 (124) pp 44-52

[13] Damien V 2012 *Fluid Mechanics and the SPH Method: Theory and Applications* (Eastbourne: Gardners Books) p 640

[14] Hoover W G 2006 *Smooth Particle Applied Mechanics: The State of the Art* (Singapour: World Scientific) p 315

[15] Mirauda D, Albano R, Sole A and Adamowski J 2020 *Smoothed Particle Hydrodynamics Modelling with Advanced Boundary Conditions for Two-Dimensional Dam-Break Floods* (MDPI, Water) № 12 (1142) p 14